Materials Chemistry and Physics 143 (2014) 1410–1416

Contents lists available at ScienceDirect

Materials Chemistry and Physics

journal homepage: www.elsevier.com/locate/matchemphys

Graphene oxide modified ZnO nanorods hybrid with high reusable photocatalytic activity under UV-LED irradiation

Kai Dai [a,*], Luhua Lu [b,*], Changhao Liang [c], Jianming Dai [c], Guangping Zhu [a], Zhongliang Liu [a], Qinzhuang Liu [a], Yongxing Zhang [a]

[a] College of Physics and Electronic Information, Huaibei Normal University, Huaibei 235000, PR China
[b] State Key Lab of Advanced Technology for Materials Synthesis and Processing, Wuhan University of Technology, Wuhan 430070, PR China
[c] Key Laboratory of Materials Physics and Anhui Key Laboratory of Nanomaterials and Nanotechnology, Institute of Solid State Physics, Hefei Institutes of Physical Science, Chinese Academy of Sciences, Hefei 230031, PR China

HIGHLIGHTS

- GO/ZnO hybrid was successfully synthesized by hydrothermal process.
- GO/ZnO hybrid showed high photocatalytic activity with irradiation of LED light.
- Effective photo-electrons separation and fast transportation.
- Excellent recycled performance was achieved by GO/ZnO hybrid.

ARTICLE INFO

Article history:
Received 29 April 2013
Received in revised form
25 September 2013
Accepted 27 November 2013

Keywords:
Nanostructures
Chemical synthesis
Electron microscopy
Oxidation

ABSTRACT

In this work, graphene oxide/zinc oxide (GO/ZnO) hybrid was prepared through a facile hydrothermal process. Transmission electron microscopy, X-ray diffraction, X-ray photoelectron spectra and N_2 adsorption and desorption isotherms were used to investigate the morphology, crystal structure, optical properties and specific surface area of GO/ZnO hybrid. It was shown that the well-dispersed ZnO nanorods were deposited on GO homogeneously. Photocatalytic properties of GO/ZnO nanorods hybrid were evaluated under 375 nm light-emitting diode light irradiation for photodegradation of methylene blue (MB). The synergic effect between GO and ZnO was found to lead to an improved photo-generated carrier separation. An optimal GO content has been determined to be 3 wt%, and corresponding the apparent pseudo-first-order rate constant k_{app} is 0.0248 min^{-1}, 4.3 times and 2.5 times more than that of pure ZnO nanorods and commercial P25 photocatalyst, respectively. Moreover, the cyclic photocatalytic test indicated that GO/ZnO hybrid can be reused for degradation of MB, suggesting the possible application of GO/ZnO hybrid as excellent candidate for water treatment.

1. Introduction

Semiconductor photocatalysts have attracted increasing attention in the past decades owing to their applications in water and air de-contamination and solar energy conversion [1–3]. Zinc oxide (ZnO), with wide band gap of 3.37 eV and large exciton binding energy of 60 meV, can act as photocatalysts for light-induced chemical transformations due to their unique electronic structure. The photogenerated holes and electrons play a very important role in pollutant degradation and photocatalytic reaction [4,5]. However, the photogenerated electron–hole pairs in the excited states are unstable and can easily recombine, which results in low photocatalytic efficiency [6–8]. During the past decade, a variety of strategies have been employed to improve the photocatalytic performance of ZnO, for example, suitable sizes and morphologies design [9,10], noble metal loading [11,12], doping [13–15], and forming semiconductor composites [16,17]. In particular, an efficient option is to design and develop hybrid materials based on ZnO to enhance their photocatalytic performance [18,19]. Zhang et al. recently reported the use of ZnO-pillared titanates for degradation of methylene blue (MB) [20], Lai et al. reported Ag doped ZnO synthesized under hydrothermal conditions and showed their enhanced photocatalytic activity for Rhodamine B [21]. Yan et al. reported alpha-Fe_2O_3/ZnO core–shell structure and showed their enhanced photocatalytic activity in aqueous solutions [22].

* Corresponding authors. Fax: +86 561 3803256.
E-mail addresses: daikai940@chnu.edu.cn, daikai940@163.com (K. Dai), lhlu@whut.edu.cn (L. Lu).

0254-0584/$ – see front matter © 2013 Elsevier B.V. All rights reserved.
http://dx.doi.org/10.1016/j.matchemphys.2013.11.055

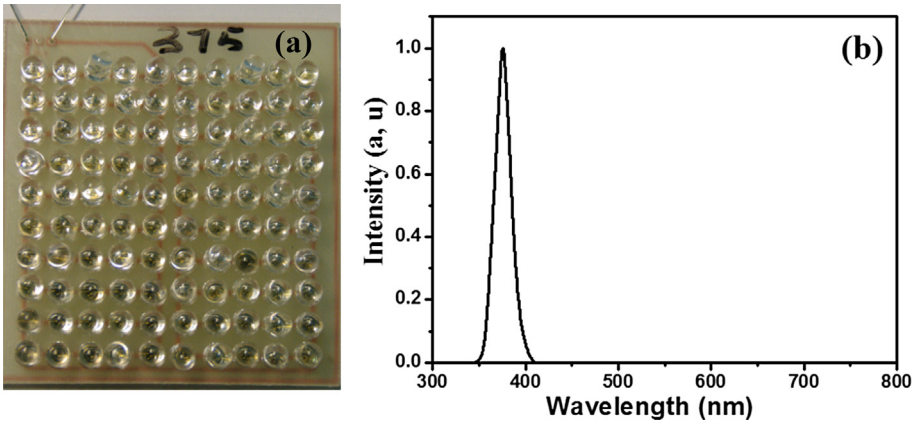

Fig. 1. (a) Photograph of LED lamps and (b) the wavelength spectrum of LED lamp.

Graphene oxide (GO) is an atomic thick nanosheet of covalently organized two-dimensional lattice of carbon atoms whose basal planes and edges are decorated with various oxygen-containing groups [23–25]. Moreover, the surface properties of GO can be adjusted through chemical modification, which favors its perfect solubility in solvents and provides fertile opportunities for the construction of GO-based hybrid nanocomposites [26–28]. So far, a paramount GO-based semiconductor photocatalysts have attracted a lot of attention due to their specific surface area, remarkable electrical conductivity, excellent adsorptivity, and high chemical and thermal stability [29–31]. Zhang et al. demonstrated graphene-P25 TiO_2 composites synthesized under hydrothermal conditions that exhibited an enhanced photocatalytic activity for the degradation of MB [32]. Zhu et al. used the water/oil system to produce GO enwrapped Ag/AgX (X = Br, Cl) composites for stable plasmonic photocatalyst [30]. Thus, the easy and large scale preparation of GO-based semiconductor photocatalysts, which simultaneously possesses superior adsorptivity, transparency, conductivity, recyclable and controllability, should be critical for the pollutants elimination and meets the demands of future environmental issues.

In this paper, we report the preparation of GO/ZnO nanorods hybrid via a simple hydrothermal method. Moreover, light-emitting diode (LED) light array was used as irradiation source, which provided the opportunity to develop small, space-saving equipment because of its compact size. The GO/ZnO nanorods hybrid exhibited an enhanced photocatalytic performance in the reduction of MB under UV-LED light irradiation as compared with that of pure ZnO nanorods and commercial P25.

2. Experimental

2.1. Materials

Natural graphite powder (325 mesh) was commercially obtained from Alfa-Aesar, TiO_2 (P25, 20% rutile and 80% anatase) was purchased from Degussa. Concentrated sulfuric acid (98%, H_2SO_4), polyethylene glycol (PEG) and potassium permanganate ($KMnO_4$) were purchased from Shanghai Chemical Reagent Co., Ltd (China). Sodium nitrate ($NaNO_3$), potassium persulfate ($K_2S_2O_8$), phosphorus pentoxide (P_2O_5), sodium sulfate (Na_2SO_4), polyvinylpyrrolidone (PVP), hydrogen peroxide (30%, H_2O_2), MB and zinc chloride ($ZnCl_2$) were purchased from Sinopharm Chemical Reagent Corp (China). All reactants were used as received without further purification. Double distilled water was used during the experimental process. The experiments were carried out at room temperature and humidity. All reactants were of analytical purity and used as received without further purification. The experiments were carried out at room temperature and humidity.

2.2. Preparation of GO

GO was synthesized by the modified Hummers' method [33,34]. In detail, 3 g of graphite was put into a mixture of 12 mL of concentrated H_2SO_4, 2.5 g of $K_2S_2O_8$, and 2.5 g of P_2O_5. The solution was heated to 80 °C and kept stirring for 4.5 h in oil bath. Then the mixture was diluted with 500 mL of deionized water, and the product was obtained by filtering using 0.2 μm Nylon film and dried under ambient condition. Thereafter, 15 g $KMnO_4$ was added gradually with stirring, to prevent the temperature of the mixture from exceeding 10 °C. The ice bath was then removed and the mixture was stirred at 35 °C for 2 h. The reaction was terminated by adding 700 mL of distilled water and 20 mL of 30% H_2O_2 solution. Finally, the GO was recovered by filtration and drying.

2.3. Preparation of GO/ZnO nanorods hybrid

6.5 g $ZnCl_2$ was initially dissolved in 100 mL distilled water followed by adding 30 mL $NH_3 \cdot H_2O$ to form a transparent solution. And then, amount of GO, 1.0 g PVP and 30 mL distilled water were added into 10 mL transparent solution to form a mixture. The mixture was further transferred into a 50 mL Teflon-lined autoclave and subsequently heated at 180 °C for 20 h. After the reaction, the

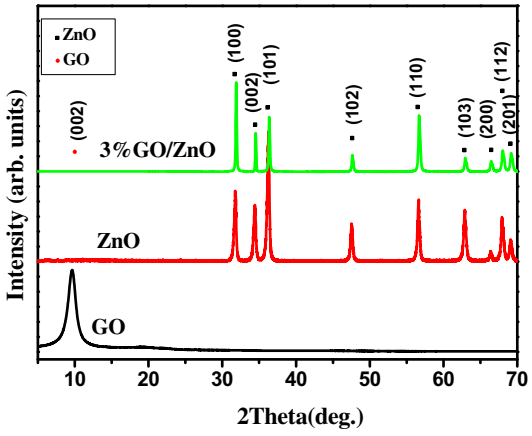

Fig. 2. XRD patterns of GO, ZnO and 3%GO/ZnO.

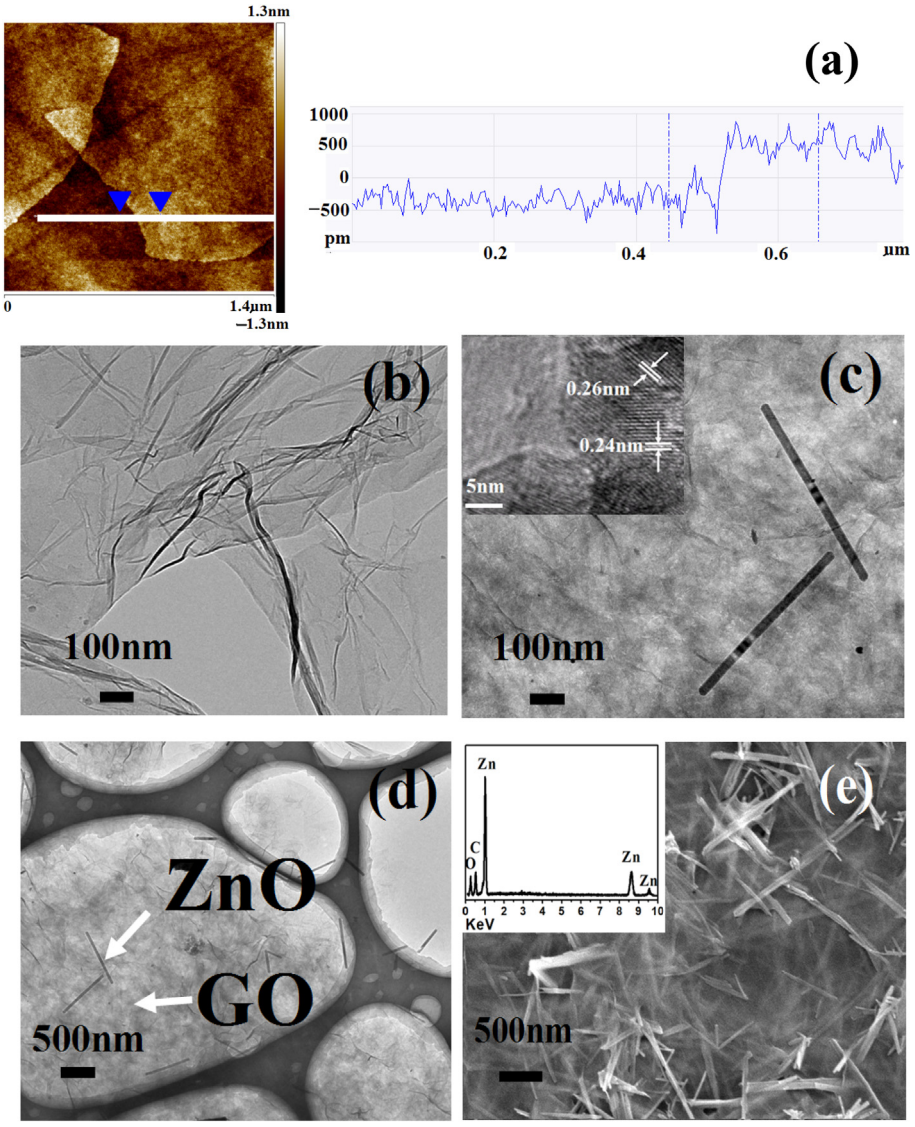

Fig. 3. AFM image of (a) GO, TEM images of (b) GO, (c) 3%GO/ZnO nanorods hybrid, low-magnification TEM image of (d) 3%GO/ZnO nanorods hybrid, and FESEM image of (e) 3%GO/ZnO nanorods hybrid. Inset in panel (e) is the EDX spectrum of 3%GO/ZnO nanorods hybrid.

products were harvested by centrifugation and throughout washing with water and ethanol, and were finally dried at 60 °C. To investigate the effect of GO content on the photocatalytic performance of GO/ZnO hybrids, the weight percentages of GO to ZnO were varied from 0 to 5 (1, 2, 3, 4, and 5 wt%) by varying the weight of GO, and the samples were presented as *x*%GO/ZnO, where *x* is the weight content of GO. ZnO nanorods were also prepared by the above-mentioned method without GO.

2.4. Analytical and testing instruments

Scanning electron microscopy (SEM) images were recorded by JSM-6700F with Inca Energy-dispersive X-ray spectroscopy (EDX). High resolution transmission electron microscopy (HRTEM) of samples was performed using Tecnai G2 F20 S-Twin. Atomic force microscopy (AFM) was conducted using a Veeco NanoScope IIIa Multimode, the frequency is 0.801 Hz, the samples were prepared by dropcasting dilute mixtures of GO sheets in ethanol onto heated, freshly cleaved mica substrates. An etched silicon tip was used as a probe to image the samples. The X-ray photoelectron spectra (XPS) of GO/ZnO hybrid were measured using a Kratos AXIS Ultra DLD X-ray photoelectron spectrometer. X-ray diffraction (XRD) data for samples were collected using a Rigaku D/MAX 24000 diffractometer with Cu Kα radiation. UV–vis diffuse reflectance spectroscopy (DRS) measurements were carried out using a Hitachi UV-3600 UV–vis spectrophotometer equipped with an integrating sphere attachment. The analysis range was from 200 to 600 nm, and $BaSO_4$ was used as reflectance standard. The Brunauer–Emmett–Teller (BET) specific surface area values were determined by using nitrogen adsorption data at 77 K obtained by a Micromeritics ASAP 2010 system with multipoint BET method. Wavelength of UV-LED was measured by PMS-50, light power was performed by UV-2000Z, voltage and current were performed by GPS-2303. The photoelectrochemical measurements were measured on CHI-660D electrochemical system, using a conventional three-electrode cell. The counter and the reference electrodes were platinum wire and saturated calomel electrode (SCE), respectively. The electrolyte solution was 0.1 M Na_2SO_4. The working electrodes were prepared as follows: the 0.25 g ground sample was mixed with 0.05 g PEG and 1 ml water was added to make slurry. The slurry was then

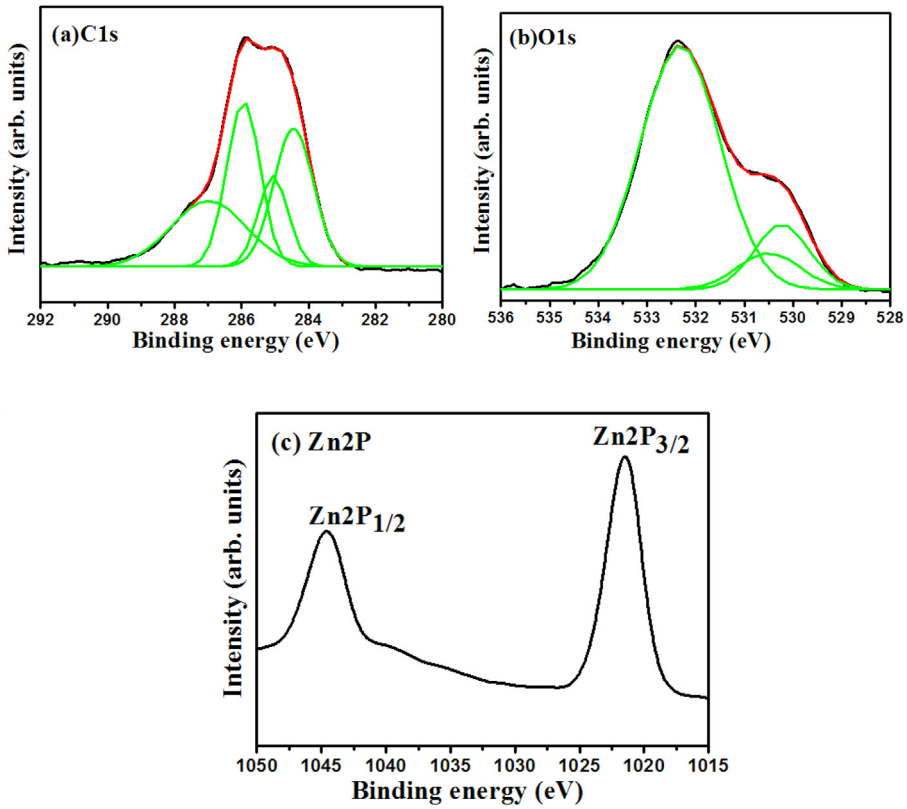

Fig. 4. XPS spectra measured at the surface of 3%GO/ZnO hybrid.

injected onto a 2.5 cm × 1.0 cm FTO glass electrode and these electrolytes were dried at 200 °C for 30 min.

2.5. Measurement of photocatalytic activity

A 10 × 10 LED array was welded on copper clad laminate, and used as light source. As indicated in Fig. 1(a), 5 LED lamps were connected in series as one group, and 20 groups in parallel were welded on copper clad laminate. Fig. 1(b) shows the wavelength spectrum of the LED at 25 °C and 20 mA. The emission center wavelength of LED is 375 nm. The photocatalytic experiments were carried out in a reactor containing the 100 mL 8 mg L^{-1} aqueous solution of MB and 0.1 g photocatalysts. The distance between the LED light source and the reactor was 1 cm. Before irradiation, the suspension was magnetically stirred in the dark for 1 h to establish adsorption equilibrium under ambient conditions. Then, the mixture was exposed to the LED light irradiation. Then, the mixture was exposed to the UV light irradiation. At the given irradiation time, the concentration of MB was quantified by the absorbance, and the absorbance wavelength used in the spectrophotometer analysis to determine MB concentration was about 664 nm. The decomposition behavior of MB by photocatalytic oxidative process can be described by Langmuir–Hinshelwood rate equation, Equation (1) can be seen as follows:

$$\frac{1}{r} = \frac{1}{k} + \frac{1}{kKC} \tag{1}$$

where C is the absorbance of the MB solution after LED light irradiation at time t; k, and K are the rate constant, and the equilibrium adsorption constant, respectively. Integrating Eq. (1) gives

$$\ln\frac{C_0}{C} = k_{app}t \tag{2}$$

where C_0 is the initial dye concentration in solution, k_{app} is the apparent pseudo-first-order rate constant, and t is the reaction time (Fig. 1).

3. Results and discussion

The XRD patterns of GO, ZnO, and 3%GO/ZnO nanorods hybrid are shown in Fig. 2. GO has a diffraction peak at 10.0°, corresponding to a (002) interplanar spacing of 8.8 Å that result from the interlamellar water trapped between hydrophilic GO sheets [35,36]. The XRD analysis further shows that the main diffraction peaks of 3%GO/ZnO hybrid are similar to that of pure ZnO and corresponds to wurtzite-structured ZnO (JPCDS 36-1451). No typical diffraction peaks of carbon species are observed due to the low amount of GO in the hybrid.

Fig. 3(a) shows AFM image of as-synthesized GO, the GO nanosheets were about 1.2 nm thick. Fig. 3(b) and (c) shows the high-magnification TEM images of as-synthesized GO and 3%GO/ZnO. It can be seen that the as-prepared GO can be dispersed well in water and the as-prepared ZnO nanorods of 3%GO/ZnO are of 20–30 nm in diameter and 500–600 nm in length. It is clearly that GO nanosheets are decorated by ZnO nanorods, which display a good combination between GO and ZnO. As indicated in the inset of Fig. 3(e), the existence of GO and ZnO in the hybrid has been proved by the peaks of C, Zn and O in EDX data.

XPS spectra of C1s, O1s and Zn2p for the 3%GO/ZnO nanorods hybrid to probe the chemical environment of the elements in the near surface range are shown in Fig. 4. Fig. 4(a) shows the high-resolution spectra of C1s, the peaks at 284.40, 285.00, 285.92 and 286.64 eV are assigned to contributions of C–C (sp^2), C–C (sp^3), C–OH, and O–C–O, respectively [37–39]. As indicated in Fig. 4(b), the binding energies of Zn 2p3/2 and 2p1/2 are centered at 1021.62 and 1044.42 eV, respectively, in agreement with those of pure ZnO [40].

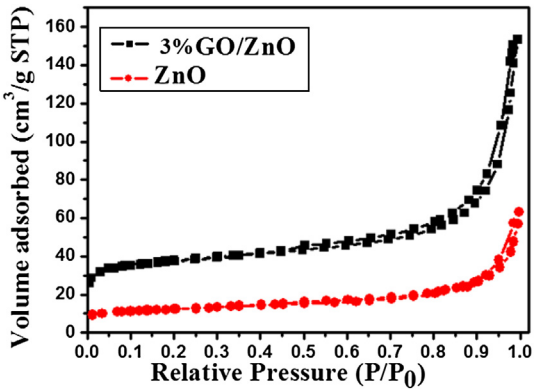

Fig. 5. The nitrogen adsorption-desorption isotherms of ZnO and 3%GO/ZnO.

Table 1
Data of BET surface area and pore specific volume of ZnO and 3%GO/ZnO.

Sample	BET ($m^2\ g^{-1}$)	Pore specific volume ($cm^3\ g^{-1}$)
ZnO	20	0.027
3%GO/ZnO	112	0.223

Fig. 4(c) shows the high-resolution spectra of O 1s. In the case of GO/ZnO hybrid, the curve fitting of O1s spectra basically indicates three components centered at 530.10, 530.62 and 532.32 eV. The peak at 530.62 eV is due to oxygen in the ZnO crystal lattice [41]. The latter two peaks are commonly ascribed to the surface oxygen complexes of carbon phase [42]. Oxygen-containing groups on the photocatalysis will lead to an increase of photocatalytic activity because the surface hydroxyl is an active species that plays an important role in semiconductor photocatalysis [43].

Fig. 5 shows the nitrogen adsorption–desorption isotherms for ZnO and 3%GO/ZnO. The data of BET surface area and pore specific volume of samples were listed in Table 1. 3%GO/ZnO hybrid displays better BET surface area and pore specific volume than that of ZnO, which should be great favor for photocatalytic performance.

During the photocatalysis, the light absorption and the charge transportation and separation are crucial factors. The DRS spectra of ZnO nanoparticles and the as-prepared 3%GO/ZnO hybrid are shown in Fig. 6. The sharp characteristic absorption edge of 3%GO/ZnO appeared at 391 nm corresponding to the indirect band gap (3.17 eV) and the baseline was increased from 391 nm to 600 nm compared to ZnO nanorods. The reason for the baseline increase of the spectra of GO/ZnO could be that the light which comes across the sample was prevented by GO sheets, which may be resulted from an increase of the surface electric charge of the oxides in the GO/ZnO hybrid and modification of the fundamental process of electron–hole pair formation during irradiation [44]. Therefore, the presence of GO nanosheets in GO/ZnO hybrid can increase the light absorption intensity and range, which results in the enhancement of the photocatalytic performance.

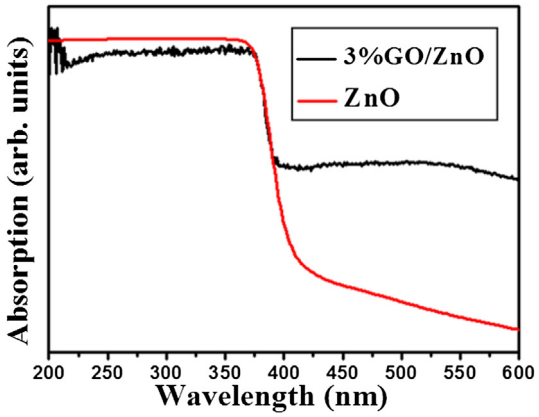

Fig. 6. UV–Vis DSR spectrum of ZnO nanorod and 3%GO/ZnO nanorods hybrid.

The photocatalytic activity of GO/ZnO nanorods hybrid was evaluated using MB as model molecules. Prior to irradiation under 375 nm LED arrays light, the solution was magnetically stirred in dark for 1 h to reach an adsorption-desorption equilibrium. The solution was then exposed to 375 nm LED arrays, the direct voltage of light array is 18.0 V and the power is 7 W. As a comparison, MB degradation with Degussa P25, ZnO nanorods and no catalyst were also carried out under same conditions. As shown in Fig. 7(a), about 6%, 12%, 9%, 13%, 21%, 23% and 26% of MB in intensity were absorbed on the ZnO nanorods, Degussa P25, 1%GO/ZnO, 2%GO/ZnO, 3%GO/ZnO, 4%GO/ZnO and 5%GO/ZnO, respectively. When the solution containing 3%GO/ZnO nanorods hybrid was irradiated with LED

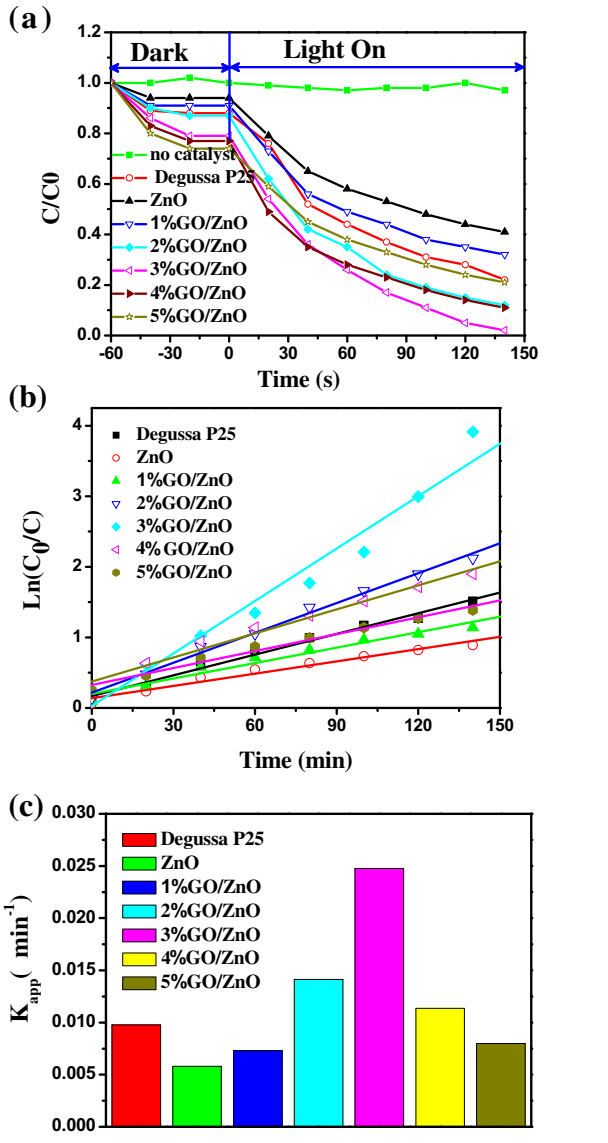

Fig. 7. Photocatalytic degradation of MB under UV light irradiation, (B) linear transform ln (C_0/C) of the kinetic curves of MB degradation over different catalysts and (c) the apparent pseudo-first-order rate constant k_{app} with different catalysts.

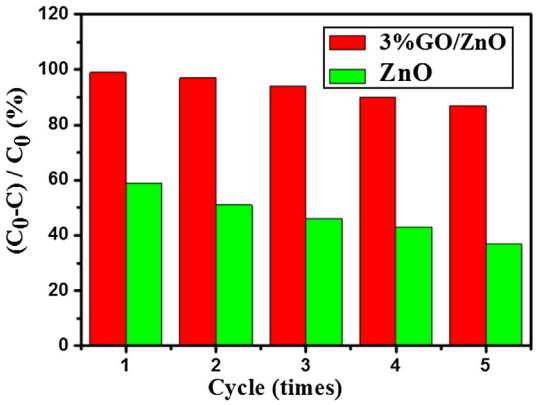

Fig. 8. Comparison of photodegradation performance within five cycles for 3%GO/ZnO nanorods hybrid and ZnO nanorod.

light, MB was nearly decomposed completely after 140 min Fig. 7(b) shows that there is a linear relationship between ln C_0/C and t, confirming that the photodegradation reaction is indeed pseudo-first-order. According to Equation (2), the apparent pseudo-first-order rate constant k_{app} with different catalysts was shown in Fig. 7(c), 3%GO/ZnO showing superior catalytic activity to commercial Degussa P25, pure ZnO nanorods and other GO/ZnO composites.

Stability of photocatalyst is an important factor for practical applications. One of the major drawbacks of ZnO photocatalysts is their severe photocorrosion under UV irradiation, which can result in significant decrease of the photocatalytic activity in reused process [45,46]. To evaluate the stability of GO/ZnO nanorods hybrid, we carried out the recycle experiment under identical conditions. Fig. 8 shows recycle experimental results of 3%GO/ZnO nanorods hybrid and ZnO nanorods, the irradiation time for each test is 140 min. As indicated in Fig. 8, the degradation efficiency of MB is about 87% and 37% in the fifth cycle for 3%GO/ZnO nanorods hybrid and ZnO nanorod photocatalyst, respectively. Moreover, the 3%GO/ZnO nanorods hybrid could be easily collected by low speed centrifugation or simple filtration over a short time, while ZnO nanorods have to be collected by longer time with higher speed centrifugation. It is obvious that GO/ZnO hybrid is a suitable photocatalyst due to its high activity and excellent recycled performance accompanied by easy separation from the reaction system.

Fig. 9 shows the proposed pathway for the photocatalytic degradation of MB molecules by the GO/ZnO hybrids. The MB molecules were captured by GO through adsorption–desorption irreversible hysteresis [47]. The large adsorption capacity was due to the large surface area of the GO. When the catalyst is irradiated with a photon of sufficient energy, equal or larger than band gap, GO may absorb the irradiation and inject the photo-induced electron into ZnO conduction band, which can trigger the formation of reactive radicals, superoxide radical ion $\cdot O^{2-}$ and hydroxyl radical ·OH, both responsible for the degradation of the organic compounds. Furthermore, inhibiting the undesirable electron–hole pair recombination is important to enhance the photocatalytic activity. Upon UV illumination, the electron–hole pairs are generated and the electrons reach the conduction band of ZnO and then transfer to the GO. Since GO behaves as conducting plane, there is no possibility of accumulation of the electrons on GO. This favors the electron–hole separation and lead to the increase of the photocurrent in the hybrid structure as the space charge effect in ZnO side becomes negligible. However, when the content of GO is further increased above its optimum value, the photocatalytic performance deteriorates. The reasons can be explained as the follows: (a) the large amount of GO can absorb some UV light and thus there exists UV light lost on ZnO, (b) some GO will act as a kind of recombination center instead of providing an electron pathway. Thus, 3%GO is the most suitable ratio for GO/ZnO catalyst in this study.

The transient photocurrent responses of the pure ZnO and 3% GO/ZnO nanorods hybrid samples were investigated for several on–off cycles of irradiation to give further evidence to support the proposed photocatalytic mechanism. As indicated in Fig. 10, steady and prompt photocurrent generation is obtained during on and off cycles of illumination. The photocurrent densities rapidly decrease to zero as soon as the lamp turns off, and the photocurrent comes back to stable values when the lamp is turned on. Under UV light irradiation, the photocurrent of the 3% GO/ZnO nanorods hybrid electrode is about four time higher than that of the pure ZnO electrode, this phenomenon indicates that more efficient photocatalytic performance for the 3%GO/ZnO nanorods hybrid samples.

Degradation efficiency of the dyes or organic compounds is highly dependent on the experimental conditions such as light irradiation source, reaction time, types of dye and weight of photocatalyst used [48]. In this work, we have used the photocatalytic reactor based on the combined use of 3%GO/ZnO photocatalyst and UV-LED light irradiation for the degradation of MB. We compared this study with the earlier reported work based on classical UV light and LED light as a source for photocatalytic degradation of MB. The comparison results are given in Table 2. Compared to different lamps such as xenon, iodine–tungsten, and mercury lamp, UV-LED sources may be a good alternative as a source for UV light irradiation for photocatalytic organic water treatment.

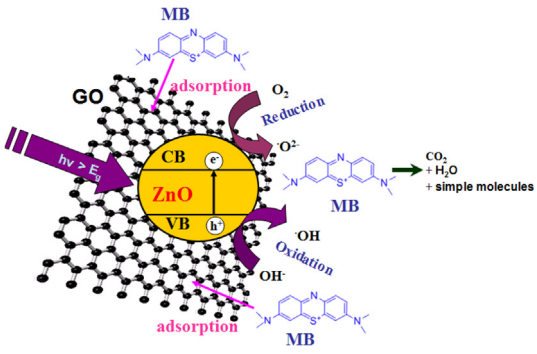

Fig. 9. Schematic of the adsorption and photocatalytic degradation of MB molecules by the GO/ZnO hybrid.

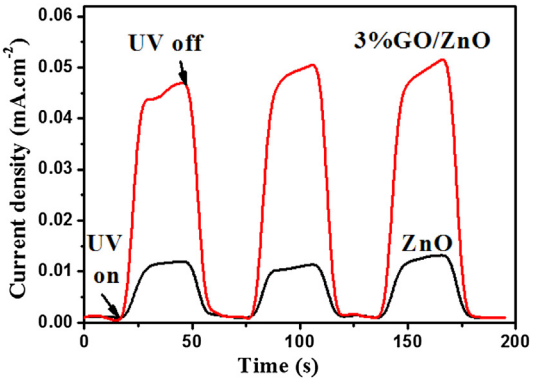

Fig. 10. Transient photocurrent responses of ZnO and 3%GO/ZnO nanorods hybrid.

Table 2
Comparison of degradation percentages of MB with literature.

No.	Catalyst	Light source	Time (min)	Degradation (%)	Ref.
1	ZnO nanoparticles	250 W high pressure mercury lamps	80	96.11	[49]
2	Beaded ZnO nanoparticles	160 W Hg lamp.	165	64	[50]
3	ZnO hollow Spheres	40 W mercury lamp	120–135	100	[10]
4	ZnO: Al	7 W UV lamp	180	90	[6]
5	ZnS nanoporous Nanoparticles	125 W high-pressure Hg lamp	40	100	[51]
6	Cu_2O	100 W iodine–tungsten lamp	180	95	[52]
7	N-doped titanate nanotubes	500 W Xenon light	300	95	[53]
8	TiO_2-quartz tubes	UV-LED (15 × 20 mW)	300	61	[48]
9	TiO_2 nanotube array	0.6 W UV-LED	300	100	[54]
10	3%GO/ZnO nanorods hybrid	7 W UV-LED	140	98	This study

4. Conclusions

In summary, high-quality GO/ZnO nanorods hybrid was synthesized by a hydrothermal method. 3%GO/ZnO hybrid exhibited a better photocatalytic performance than that of pure ZnO and Degussa P25 under 375 nm LED light irradiation. The improved photocatalytic performance could be ascribed to the high BET surface area of hybrid for capturing MB molecules, and the reduction of photoelectron–hole pair recombination with GO as conducting plane. Considering the ease separation, recycling, mass production of GO/ZnO hybrid, it should be a promising candidate materials for pollutant elimination applications.

Acknowledgments

This work was supported by the National Natural Science Foundation of China (51302101, 21303129, 11004071), the Key Foundation of Educational Commission of Anhui Province (KJ2012A250), the Natural Science Foundation of Anhui Province (11040606M10, 11040606M64), and the Huaibei Science and Technology Development Funds (20110305).

References

[1] J. Tao, T. Luttrell, M. Batzill, Nat. Chem. 3 (2011) 296–300.
[2] H. Tong, S. Ouyang, Y. Bi, N. Umezawa, M. Oshikiri, J. Ye, Adv. Mater. 24 (2012) 229–251.
[3] X. .Chen, S.S. Mao, Chem. Rev. 107 (2007) 2891–2959.
[4] M.R. Hoffmann, S.T. Martin, W. Choi, D.W. Bahnemannt, Chem. Rev. 95 (1995) 69–96.
[5] S. Xu, Z.L. Wang, Nano Res. 4 (2011) 1013–1098.
[6] M. Bizarro, A. Sánchez-Arzate, I. Garduño-Wilches, J.C. Alonso, A. Ortiz, Catal. Today 166 (2011) 129–134.
[7] I. Shalish, H. Temkin, V. Narayanamurti, Phys. Rev. B 69 (2004) 245401.
[8] Y. Li, F. Della Valle, M. Simonnet, I. Yamada, J.J. Delaunay, Appl. Phys. Lett. 94 (2009) 023110.
[9] F. Lu, W. Cai, Y. Zhang, Adv. Funct. Mater. 18 (2008) 1047–1056.
[10] Z. Deng, M. Chen, G. Gu, L. Wu, J. Phys. Chem. B 112 (2008) 16–22.
[11] Y. Zheng, C. Chen, Y. Zhan, X. Lin, Q. Zheng, K. Wei, J. Zhu, J. Phys. Chem. C 112 (2008) 10773–10777.
[12] Y.H. Sung, V.D. Frolov, S.M. Pimenov, J.J. Wu, Phys. Chem. Chem. Phys. 14 (2012) 14492–14494.
[13] Y.G. Lin, Y.K. Hsu, Y.C. Chen, L.C. Chen, S.Y. Chen, K.H. Chen, Nanoscale 4 (2012) 6515–6519.
[14] A. Kovalenko, G. Pourroy, O. Cregut, M. Gallart, B. Hönerlage, P. Gilliot, J. Phys. Chem. C 114 (2010) 9498–9502.
[15] L.W. Sun, H.Q. Shi, W.N. Li, H.M. Xiao, S.Y. Fu, X.Z. Cao, Z.X. Li, J. Mater. Chem. 22 (2012) 8221–8227.
[16] X. Liu, X. Wang, H. Li, L. Pan, T. Lv, Z. Sun, C. Sun, J. Mater. Chem. 22 (2012) 16293–16298.
[17] H. Zhou, S.S. Wong, ACS Nano 2 (2008) 944–958.
[18] K. Dai, G. Dawson, S. Yang, Z. Chen, L. Lu, Chem. Eng. J. 191 (2012) 571–578.
[19] P. Li, Z. Wei, T. Wu, Q. Peng, Y. Li, J. Am. Chem. Soc. 133 (2011) 5660–5663.
[20] K.Z. Zhang, B.Z. Lin, Y.L. Chen, B.H. Xu, X.T. Pian, J.D. Kuang, B. Li, J. Colloid Interface Sci. 358 (2011) 360–368.
[21] Y. Lai, M. Meng, Y. Yu, Appl. Catal. B: Environ. 100 (2010) 491–501.
[22] W. Yan, H. Fan, C. Yang, Mater. Lett. 65 (2011) 1595–1597.
[23] A. Kubacka, M. Fernández-García, G. Colón, Chem. Rev. 112 (2012) 1555–1614.
[24] Z. Sun, D.K. James, J.M. Tour, J. Phys. Chem. Lett. 2 (2011) 2425–2432.
[25] B.J. Hong, O.C. Compton, Z. An, I. Eryazici, S.T. Nguyen, ACS Nano 6 (2012) 63–73.
[26] B. Adhikari, A. Biswas, A. Banerjee, ACS Appl. Mater. Inter. 4 (2012) 5472–5482.
[27] Z. Tang, H. Chen, X. Chen, L. Wu, X. Yu, J. Am. Chem. Soc. 134 (2012) 5464–5467.
[28] Y. Liang, H. Wang, J. Zhou, Y. Li, J. Wang, T. Regier, H. Dai, J. Am. Chem. Soc. 134 (2012) 3517–3523.
[29] S. Wang, C.T. Nai, X.F. Jiang, Y. Pan, C.H. Tan, M. Nesladek, Q.H. Xu, K.P. Loh, J. Phys. Chem. Lett. 3 (2012) 2332–2336.
[30] M. Zhu, P. Chen, M. Liu, ACS Nano 5 (2011) 4529–4536.
[31] G. Williams, B. Seger, P.V. Kamat, ACS Nano 2 (2008) 1487–1491.
[32] H. Zhang, X.J. Lv, Y.M. Li, Y. Wang, J.H. Li, ACS Nano 4 (2010) 380–386.
[33] W.S. Hummers, R.E. Offeman, J. Am. Chem. Soc. 80 (1958), 1339–1339.
[34] Y. Wang, Y.M. Li, L.H. Tang, J. Lu, J.H. Li, Electrochem. Commun. 11 (2009) 889–892.
[35] D.A. Dikin, S. Stankovich, E.J. Zimney, R. Piner, G.H.B. Dommett, G. Evmenenko, S.T. Nguyen, R.S. Ruoff, Nature 448 (2007) 457–460.
[36] S. Park, J. An, I. Jung, R.D. Piner, S.J. An, X. Li, A. Velamakanni, R.S. Ruoff, Nano Lett. 9 (2009) 1593–1597.
[37] Z. Zhan, L. Zheng, Y. Pan, G. Sun, L. Li, J. Mater. Chem. 22 (2012) 2589–2595.
[38] S. Akbar, S.K. Hasanain, M. Abbas, S. Ozcan, B. Ali, S.I. Shah, Solid State Commun. 151 (2011) 17–20.
[39] S.T. Tan, X.W. Sun, Z.G. Yu, P. Wu, G.Q. Lo, D.L. Kwong, Appl. Phys. Lett. 91 (2007) 072101.
[40] H.K. Kim, K.K. Kim, S.J. Park, T.Y. Seong, I. Adesida, J. Appl. Phys. 94 (2003) 4225–4227.
[41] X.Q. Wei, B.Y. Man, M. Liu, C.S. Xue, H.Z. Zhuang, C. Yang, Physica B 388 (2007) 145–152.
[42] J. Mu, C. Shao, Z. Guo, Z. Zhang, M. Zhang, P. Zhang, B. Chen, Y. Liu, ACS Appl. Mater. Inter. 3 (2011) 590–596.
[43] B. Xin, L. Jing, Z. Ren, B. Wang, H. Fu, J. Phys. Chem. B 109 (2005) 2805–2809.
[44] J. Zhang, X. Xu, Z.F. Feng, M.J. Li, C. Li, Angew. Chem. Int. Ed. 47 (2008) 1766–1769.
[45] H. Fu, T. Xu, S. Zhu, Y. Zhu, Environ. Sci. Technol. 42 (2008) 8064–8069.
[46] Y. Wang, R. Shi, J. Lin, Y. Zhu, Energy Environ. Sci. 4 (2011) 2922–2929.
[47] J. Liu, Z. Wang, L. Liua, W. Chen, Phys. Chem. Chem. Phys. 13 (2011) 13216–13221.
[48] K. Natarajan, T.S. Natarajan, H.C. Bajaj, R.J. Tayade, Chem. Eng. J. 178 (2011) 40–49.
[49] S.B. Khan, M. Faisal, M.M. Rahman, A. Jamal, Talanta 85 (2011) 943–949.
[50] M. Dutta, D. Basak, Nanotechnology 20 (2009) 475602.
[51] J.S. Hu, L.L. Ren, Y.G. Guo, H.P. Liang, A.M. Cao, L.J. .Wan, C.L. Bai, Angew. Chem. Int. Ed. 44 (2005) 1269–1273.
[52] L. Xu, H. Xu, S. Wu, X. Zhang, Appl. Surf. Sci. 258 (2012) 4934–4938.
[53] C.C. Hu, T.C. Hsu, S.Y. Lu, Appl. Surf. Sci. 280 (2013) 171–178.
[54] T.S. Natarajan, K. Natarajan, H.C. Bajaj, R.J. Tayade, Ind. Eng. Chem. Res. 50 (2011) 7753–7762.